

Self-starting and self-Q-switching dynamics of passively mode-locked Nd:YLF and Nd:YAG lasers

U. Keller, T. H. Chiu, and J. F. Ferguson

AT&T Bell Laboratories, Crawfords Corner Road, Holmdel, New Jersey 07733

Received August 12, 1992

The semiconductor antiresonant Fabry-Perot saturable absorber (A-FPSA) has a bitemporal absorption response with a slow time component that is due to carrier recombination and a fast time component that is due to intraband thermalization. We demonstrate that the slow component provides the self-starting mechanism and without significant Kerr lens contribution the fast component is necessary for steady-state pulse formation in passively cw mode-locked solid-state lasers. The carrier lifetime of the bitemporal A-FPSA was varied by the molecular-beam-epitaxy growth temperature to characterize its influence on the self-starting and self-Q-switching dynamics of cw mode-locked Nd:YLF and Nd:YAG lasers. The A-FPSA carrier lifetime and the top reflector of the A-FPSA can be adjusted to optimize the self-starting performance and to prevent self-Q-switching of cw mode-locked solid-state lasers.

In previous studies we introduced the intracavity antiresonant Fabry-Perot saturable absorber (A-FPSA) (Fig. 1), which is to our knowledge the first passive intracavity mode locker that both starts and sustains stable mode locking without self-Q-switching of a cw-pumped Nd:YLF (Ref. 1) and Nd:YAG (Ref. 2) laser. Operation of a Fabry-Perot saturable absorber at antiresonance with a high reflectivity of the top mirror strongly decreases the intensity inside the Fabry-Perot cavity with respect to the incident intensity. This transforms the saturable absorber to a high-saturation-intensity, low-loss absorber. The A-FPSA, which consists of a low-temperature molecular-beam-epitaxy (MBE) grown InGaAs/GaAs saturable absorber, has a bitemporal absorption bleaching response with a slow time component that is due to carrier recombination and a fast time component that is due to intraband thermalization.³ The slow time constant can be continuously changed with the MBE growth temperature.

We show in this Letter that the slow component of the bitemporal A-FPSA provides the self-starting mechanism without self-Q-switching. Because Kerr lens mode locking (KLM) contributions are estimated to be small, our experimental results imply that the fast component is necessary for steady-state pulse formation owing to the lack of significant gain saturation.⁴ In contrast, KLM is based on a fast saturable absorber alone and is not self-starting.^{5,6} A KLM Nd:YLF laser required an additional starting mechanism, such as an acousto-optic modulator, to initiate mode locking.⁷

The experimental setup consists of the following: The laser cavity is a linear folded end-pumped configuration with an intracavity A-FPSA for passive mode locking.^{1,2} The saturable absorber layer in the A-FPSA is an InGaAs/GaAs multiple-quantum-well layer ($0.61 \mu\text{m}$ thick) with a band-gap wavelength of $\approx 1.05 \mu\text{m}$ and is grown at low temperatures (LT) on top of the GaAs/AlAs dielectric mirror. The MBE growth temperature was set at 200, 260, 315, and 340°C to produce samples with measured carrier

lifetimes of $< 3, 8, 17,$ and 30 ps, respectively. Finally, a $\text{TiO}_2/\text{SiO}_2$ dielectric mirror with a 98% or 95% reflectivity (R_1 in Fig. 1) is evaporated onto the absorber layer. All samples were coated at the same time to ensure uniformity.

Both the Nd:YLF and the Nd:YAG lasers are pumped with a cw Ti:sapphire laser. Using a 2% output coupler, we typically achieved pump thresholds ~ 10 mW and a slope efficiency of 33% and 40%, respectively. The cavity round-trip small-signal gain is determined by $G_0 \approx (2\pi)^2 T \tau_g f_{\text{relax}}^2$ for a pump power far above threshold, where f_{relax} is the measured relaxation oscillation frequency, $\tau_g \approx 450 \mu\text{s}$ is the upper-state lifetime of the Nd:YLF laser, and $T = 4.5$ ns is the cavity round-trip time. For example, with 0.8 W of pump power and $f_{\text{relax}} = 195$ kHz, G_0 is ≈ 3 (i.e., 300%).

We used an intracavity mechanical chopper to study the self-starting dynamics and monitor both the average power and the second-harmonic generation (SHG) signal. The delay of the second-harmonic signal determines the mode-locking buildup time. The average buildup time of a stable cw mode-locked Nd:YLF laser (no self-Q-switching) is summarized in Fig. 2. Both the laser mode inside the gain medium and on the saturable absorber are kept constant for each A-FPSA sample by maintaining the same pulse repetition rate (i.e., cavity length) throughout all measurements. In comparison, similar measurements determined a $200\text{-}\mu\text{s}$ buildup time for passively mode-

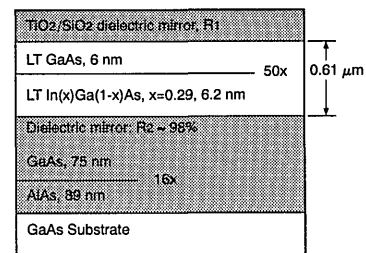


Fig. 1. Bitemporal A-FPSA: The reflectivity of the top mirror R_1 is 98% or 95%.

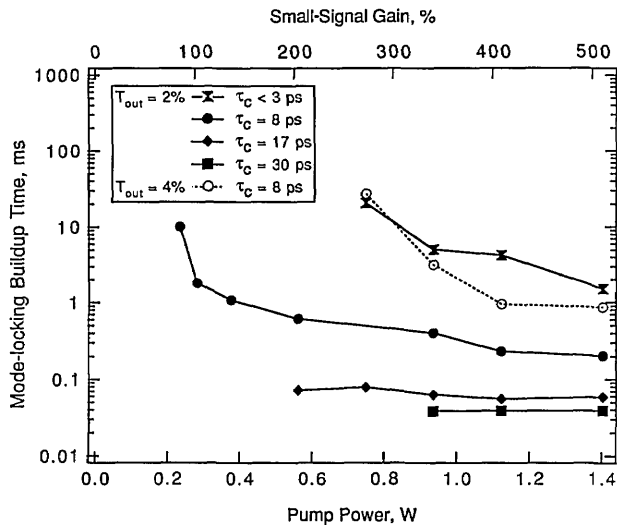


Fig. 2. Starting dynamics of the Nd:YLF laser (without self- Q -switching) using a bitemporal A-FPSA ($R_1 = 98\%$) with different carrier lifetimes τ_c .

locked Ti:sapphire lasers^{8,9} and a 15- μ s buildup time for a colliding-pulse mode-locked dye laser.¹⁰

Figure 2 clearly shows that the mode-locking buildup time decreases for longer carrier life times. This can be explained as follows: The saturable absorber is more strongly bleached at pulsed operation, which can be modeled with nonlinear absorption coefficient

$$\frac{\alpha_s}{1+x} + \alpha_{ns}, \quad (1)$$

where α_s is the part of the absorption coefficient that can be saturated, α_{ns} is the part that cannot be saturated (such as scattering losses), and x determines the absorption bleaching with $x = x_{cw}$ at cw operation and $x = x_p$ at pulsed operation¹¹:

$$x_{cw} = \frac{P}{P_a} = P \frac{\sigma_a \tau_c}{A_a h \nu}, \quad x_p = x_{cw} \frac{T}{\tau_c}, \quad (2)$$

where P is the average intracavity power at steady state, P_a is the average saturation power of the saturable absorber (i.e., A-FPSA), σ_a is the saturable absorber cross section that depends on R_1 (Fig. 1), τ_c is the carrier lifetime of the A-FPSA, A_a is the laser mode area on the A-FPSA, $h\nu$ is the photon energy, and $T \approx 4.5$ ns is the cavity round-trip time. In Eqs. (2) we assumed that the steady-state pulse duration τ_p is smaller than τ_c , which implies no significant carrier recombination during the pulse duration. To minimize bleaching at cw operation (i.e., $x_{cw} \ll 1$), σ_a has to be chosen to be relatively small, which requires a high top reflector of the semiconductor A-FPSA. Because $T/\tau_c \gg 1$, the bleaching at pulsed operation is strongly increased [Eqs. (2)]. Initially during the mode-locking buildup, the mode-beating fluctuations $\delta P(t)$ have low powers and long durations. The mode-beating pulses grow because they increase the bleaching in the saturable absorber by

$$\delta x \sim \int \delta P(t) \exp\left(-\frac{t}{\tau_c}\right) dt, \quad (3)$$

which reduces their loss. Therefore, these initial noise fluctuations grow faster with a longer τ_c . In addition, as expected, a shorter buildup time is observed with a higher small-signal gain or a longer cavity lifetime (i.e., lower loss) (Fig. 2). For example, with a Nd:YAG laser, which has a higher gain cross section than the Nd:YLF laser, the mode-locking buildup time was reduced to 33 μ s for the 17-ps carrier lifetime sample at an absorbed pump power of 1.1 W.

There is a trade-off: A longer carrier lifetime reduces the buildup time (Fig. 2) but increases the tendency for self- Q -switching. This is more severe the longer the upper-state lifetime of the laser material. To achieve a quantitative measure for the self- Q -switching we use a photodetector with a microwave spectrum analyzer.¹ In the frequency domain of the detected laser intensity, the mode-locked pulses produce laser harmonics at multiples of the pulse repetition rate ≈ 220 MHz and the relaxation oscillations produce noise sidebands that peak at the relaxation oscillation frequency with a certain number of dBc below the laser harmonic. Self- Q -switching produces very strong modulation sidebands (typically near -1 dBc) at the relaxation oscillation frequency.¹ The use of a microwave spectrum analyzer allows a quantitative measure of how well the laser is mode locked.

Figure 3 shows that the carrier lifetime of the A-FPSA ($R_1 = 98\%$) strongly affects the strength of the relaxation oscillations for the Nd:YLF laser with a 2% output coupler. When the pump power is increased the laser goes from increased mode-beating noise without stable autocorrelation traces to stable self- Q -switching, where stable mode-locked pulses are formed within a Q -switched pulse envelope of ≈ 2 - μ s duration, and finally to stable mode locking, where the relaxation oscillations are approximately more than 30 dB below the laser harmonic. For longer carrier lifetimes, the tendency for self- Q -switching is increased and higher pump power is required for stable mode locking (Fig. 3). Increasing the output coupler to 4% increases the strength of the relaxation oscillations: For the A-FPSA with an 8-ps carrier lifetime the relaxation oscillations typically increases by 10 to 20 dB, whereas for A-FPSA's with the longer carrier lifetimes self- Q -switching could not be prevented with a pump power of < 1.7 W. Furthermore, when we used a lower absorber cross section (an A-FPSA with $R_1 = 95\%$) we could not prevent self- Q -switching at all. In contrast, with a Nd:YAG laser, which has a shorter upper-state lifetime, the tendency for self- Q -switching is strongly reduced, and we even obtained stable mode locking using A-FPSA's with $R_1 = 95\%$.

Our observations for the tendency of self- Q -switching are consistent with Haus's condition to prevent self- Q -switching instabilities¹² (assuming negligible gain saturation):

$$\delta_a \frac{P}{P_a} < \frac{T}{\tau_g} \left(1 + \frac{P}{P_a}\right)^2, \quad (4)$$

where τ_g is the upper-state lifetime of the laser

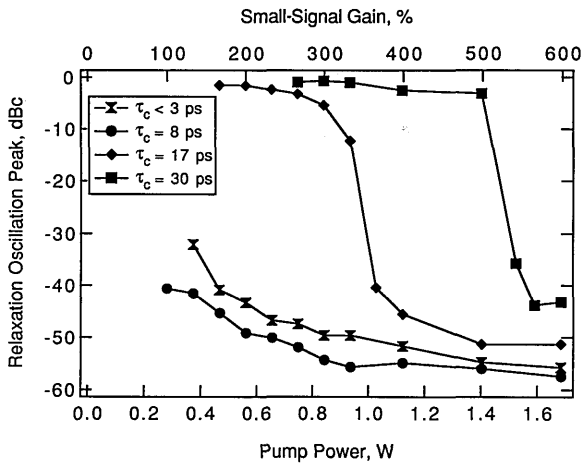


Fig. 3. Self- Q -switching behavior of the Nd:YLF laser. Values are only given when mode locking is self-starting and a stable autocorrelation is observed.

medium and δ_a is the unsaturated loss coefficient of the A-FPSA.

The steady-state pulse duration decreases with increased pump power but does not strongly depend on the carrier lifetime. For the Nd:YLF laser pulses as short as 2.8 ps and for the Nd:YAG laser pulses as short as 7 ps are generated assuming a sech² pulse shape. Previously, we have demonstrated with a resonant passive mode-locked Nd:YLF laser (same pump geometry and similar cavity parameters) that by blocking the coupled cavity the laser immediately falls back into cw operation.¹³ Therefore owing to the direct analogy between resonant passive mode locking and the A-FPSA,^{1,6} self-focusing effects are too small to self-sustain mode locking in our case. $ABCD$ matrix calculations showed that the Kerr-induced change of the beam waist in the laser rod is $< 0.1 \mu\text{m}$ assuming a cavity mode waist of $120 \mu\text{m} \times 60 \mu\text{m}$.² In addition, because the laser was always optimized for maximum power and the pump beam waist of $20 \mu\text{m}$ is significantly smaller than the cavity mode, we would not expect significant KLM because of gain aperturing. However, we obtain mode-locked pulse durations of 3 ps even with A-FPSA samples with a carrier lifetime of ≥ 30 ps. This indicates that at steady state the fast component of the bitemporal A-FPSA becomes the dominant pulse-forming mechanism. With shorter pulse durations and higher peak powers KLM is expected to dominate at steady state, and the A-FPSA will only act as a passive starting mechanism.⁶

In summary, more stable mode locking is achieved with the following [relation (4)]: higher small-signal gain (i.e., higher pump power), shorter upper-state lifetime of the gain material τ_g , lower intracavity losses, and larger average saturation power P_a . For example, P_a can be increased by increasing R_1 of the A-FPSA (Fig. 1), by increasing A_a ,² or by reducing the carrier lifetime τ_c of the A-FPSA [Eqs. (2)]. A high- Q cavity is essential for stable mode locking. Therefore, using a relatively high R_1 on the A-FPSA to minimize intracavity losses,

we can increase τ_c for efficient self-starting without affecting the Q of the cavity but with an upper limit determined by the onset of self- Q -switching. Owing to the high small-signal gain achieved with Ti:sapphire laser pumping, the Nd:YLF laser is still self-starting even with a small τ_c [i.e., $\tau_c < \tau_p$ in Fig. 2(b)], however, the relaxation oscillation noise is increased (Fig. 3) because the mode-locking buildup time becomes too long. If the relaxation oscillations are not strongly damped, the laser tends to self- Q -switch briefly after the initial mode-locking buildup time. This produces some fluctuations (< 100 ms) in both the average output power and the second-harmonic signal.

In conclusion, we have characterized the starting and the self- Q -switching dynamics of Nd:YLF and Nd:YAG lasers using a bitemporal A-FPSA. The A-FPSA carrier lifetime was adjusted to optimize the self-starting performance with both Nd:YLF and Nd:YAG without self- Q -switching. Given a certain laser material, laser cavity design, and available pump power, the saturable absorber parameters such as saturable absorber cross section, loss, and recovery time (i.e., carrier lifetime) can be independently designed for stable self-starting mode locking without self- Q -switching. The absorption edge of the A-FPSA can be varied by adjusting the semiconductor's band-gap energy, which allows extension of this technique to other laser materials and wavelengths.

References

1. U. Keller, D. A. B. Miller, G. D. Boyd, T. H. Chiu, J. F. Ferguson, and M. T. Asom, *Opt. Lett.* **17**, 505 (1992).
2. U. Keller, D. A. B. Miller, G. D. Boyd, T. H. Chiu, J. F. Ferguson, and M. T. Asom, in *Advanced Solid-State Lasers*, Vol. 13 of OSA Proceedings Series, L. Chase and A. Pinto, eds. (Optical Society of America, Washington, D.C., 1992), p. 98.
3. T. B. Norris, W. Sha, W. J. Schaff, X. J. Song, Z. Lilienthal-Weber, and E. R. Weber, in *Picosecond Electronics and Optoelectronics*, Vol. 9 of OSA Proceedings Series, T. C. L. Sollner and J. Shah, eds. (Optical Society of America, Washington, D.C., 1991), p. 244.
4. H. A. Haus, U. Keller, and W. H. Knox, *J. Opt. Soc. Am. B* **8**, 1252 (1991).
5. D. E. Spence, P. N. Kean, and W. Sibbett, *Opt. Lett.* **16**, 42 (1991).
6. U. Keller, W. H. Knox, and G. W. 'tHooft, *IEEE J. Quantum Electron.* **28**, 2123 (1992).
7. G. P. A. Malcolm and A. I. Ferguson, *Opt. Lett.* **16**, 1987 (1991).
8. J. Goodberlet, J. Wang, J. G. Fujimoto, and P. A. Schulz, *Opt. Lett.* **15**, 1300 (1990).
9. N. Sarukura and Y. Ishida, *Opt. Lett.* **17**, 61 (1992).
10. J.-C. Kuo and C.-L. Pan, *Opt. Lett.* **15**, 1297 (1990).
11. U. Keller, L. E. Nelson, and T. H. Chiu, in *Advanced Solid-State Lasers*, Vol. 13 of OSA Proceedings Series, L. Chase and A. Pinto, eds. (Optical Society of America, Washington, D.C., 1992), p. 94.
12. H. A. Haus, *IEEE J. Quantum Electron.* **QE-12**, 169 (1976), Eq. 28.
13. U. Keller and T. H. Chiu, *IEEE J. Quantum Electron.* **28**, 1710 (1992).